Soils and Foundations 2015;55(5):1196–1210

HOSTED BY

CrossMark

ELSEVIER

The Japanese Geotechnical Society

Soils and Foundations

www.sciencedirect.com
journal homepage: www.elsevier.com/locate/sandf

SOILS AND FOUNDATIONS

Dynamics of potential fill–backfill material at very small strains

K. Senetakis[a,*], B.N. Madhusudhan[b]

[a]University of New South Wales, Sydney, Australia
[b]University of Southampton, Southampton, UK

Received 24 September 2014; received in revised form 21 April 2015; accepted 22 May 2015
Available online 26 September 2015

Abstract

The paper presents a synthesis of past and recently acquired laboratory test results on granular soils using wave propagation techniques at very small strain amplitudes. Resonant column tests on uniform to well-graded coarse sands and gravels of angular and low sphericity grains were analyzed. Empirical-type equations were developed for the prediction of the elastic modulus and material damping at small strains considering the effects of the grading characteristics, the isotropic effective stress and the void ratio. The G_0–p' relationship, expressed through ~~exponent~~ n_G, was affected by the sample preparation method. For the narrow range in relatively low pressures adopted in the study, it was observed that n_G decreased slightly with an increase in relative density. Due to the limited initial void ratios of those tests, the effect of the preparation method was not incorporated into the proposed formulae for the n_G prediction. In this direction, additional experiments from the literature, which adopted the resonant column and bender element methods, were further analyzed, including soils of variable types tested with a wider range in relative densities. By employing typical formulae from the theory of elasticity, the bulk modulus and the changes in void ratio were estimated based on the change in isotropic effective stress in the literature data. Considering the recent micromechanical experimental findings associated with the nature of the contact response of soil particles, the importance of soil type and particle-contact behavior in the constant-state response of soils was demonstrated and quantified. Material damping values ranged from about 1.10% to about 0.45% for p' from 25 to 200 kPa with a slight decrease in D_{s0} with an increase in pressure.

Keywords: Resonant column; Bender elements; Dry sand; Shear modulus; Damping ratio; Elastic properties

1. Introduction

The resonant column method provides reliable measurements of modulus and damping at very small to medium strains, within a range of about 10^{-4}–10^{-2}%. Modulus derivations refer to secant stiffness and can provide an excellent indication of fabric effects. Constant-state stiffness and material damping are pressure-dependent and the G_0–p' and D_{s0}–p' relationships are expressed through Eqs. (1) and (2), where G_0 and D_{s0} are the small-strain shear modulus and the material damping, respectively, and p' is the isotropic effective stress. The power n_G and n_D in these formulae express the effect of p' in the constant-state properties of soils, whilst A_G and A_D are material-dependent constants (Santamarina and Cascante, 1998; Santamarina et al., 2001). With reference to dry granular soils, material damping at very small strains is not affected significantly by the loading frequency (Menq, 2003); and thus, derivations for energy losses may also be considered in the resonant column method without any considerable effect of viscous damping on dry sands or gravels.

$$G_0 = A_G \times (p')^{n_G} \quad (1)$$

*Corresponding author.
E-mail address: k.senetakis@unsw.edu.au (K. Senetakis).
Peer review under responsibility of The Japanese Geotechnical Society.

http://dx.doi.org/10.1016/j.sandf.2015.09.019

$$D_{s0} = A_D \times (p')^{n_D} \tag{2}$$

Past and recently acquired research works have demonstrated that resonant column test results may also provide useful information related to the effect of properties at the grain scale on the macro-scale response of soils and a better understanding of the dominant mechanisms in particulate media during cyclic/dynamic loading (e.g., Santamarina and Cascante, 1996, 1998; Cascante and Santamarina, 1996; Senetakis et al., 2013a, 2013b). This is because the resonant column method provides an indication of the fabric effects even in the range of extremely small deformations (e.g., Cascante and Santamarina, 1996), and these fabric effects, from a micromechanical point of view, are linked to the magnitude and the distribution of the contact forces (e.g., Radjai and Wolf, 1998) and the probable preferable concentration of normals in the vertical direction within a granular assembly of particles (e.g., Yoshimine et al., 1998). For example, it has been shown through resonant column tests that due to the plastic nature of the particle contact response, which is more dominant in the sliding direction (e.g., micromechanical experimental findings by Cole and Peters, 2007, 2008, Cole et al., 2010, and Senetakis et al., 2013c), the G_0–p' relationship cannot be described efficiently by the Hertz–Mindlin theory. This theory could predict a value for the exponent n_G equal to 1/3 (Santamarina and Cascante, 1996), which represents more effectively particulate media with an elastic particle-contact response in nature. However, higher values for n_G have been determined through resonant column tests or derived from other wave propagation techniques, such as the bender element method or cyclic-dynamic triaxial tests (e.g., Hardin and Richart, 1963, Hardin, 1978, Kokusho, 1980, Chung et al., 1984, Tanaka et al., 1987, Goto et al., 1987, Menq, 2003, Cho et al., 2006, Senetakis et al., 2012 among others). This is because of the visco-plastic to brittle nature of the contact response of soil particles (Cascante and Santamarina, 1996).

Through wave propagation experiments, Cho et al. (2006) found a significant effect of particle shape in the G_0–p' relationship. They attributed their observations to the possible effect of the particle contact response which alters between irregular and regular in shape particles, perhaps because of the more pronounced grain crushing or micro-crushing and overall changes in bulk volume when more irregularly shaped particles are considered than regularly shaped particles. Through one-dimensional compression tests on reference particles, Cavarretta et al. (2010) verified the significant effect of particle shape in the overall compression-pressure relationship which, in turn, affects the fabric, and thus, the stiffness of geo-materials. In this direction, Senetakis et al. (2012), who studied the small-strain dynamic properties of fine- to medium-grained sands, reported a significant effect of particle shape on the constants n_G and A_G.

Menq (2003) and Menq and Stokoe (2003) noticed in their resonant column experiments a dominant effect of the coefficient of uniformity in the G_0–p' relationship. This trend has been correlated, partly, through numerical simulations and quantification of the grain size distribution effects on isotropically consolidated granular assemblies, to the distribution and magnitude of the particle contact forces (e.g., Radjai and Wolf, 1998, Radjai et al., 1998). Recently, Senetakis et al. (2012, 2013a) highlighted the importance of particle type and morphology in the G_0–p' relationship. Senetakis et al. attributed their observations primarily to the possibly more pronounced damage of surface roughness because of the coupled normal force – deflection and tangential force – deflection responses at particle contacts. These derivations were based on the recent quantification of particle damage by Senetakis et al. (2013c) and measurements of friction and stiffness at particle contacts by Senetakis et al. (2013c, 2013d) and Senetakis and Coop (2014, 2015) on reference strong particles of a quartz sand and reference weak particles of a biogenic crushable sand. For example, Fig. 1 presents the coupled effect of normal load and tangential load – deflection responses at the contacts of two quartz particles before and after sliding tests by Senetakis et al. (2013c). In this figure, a cross-section of a quartz particle is shown within the area of contact and sliding on the surface of another similar particle before and after micromechanical sliding tests. They quantified the damage of the surface roughness using white light interferometry. As demonstrated in the figure, the coupled effect of the normal force and sliding significantly reduced the magnitude of surface roughness

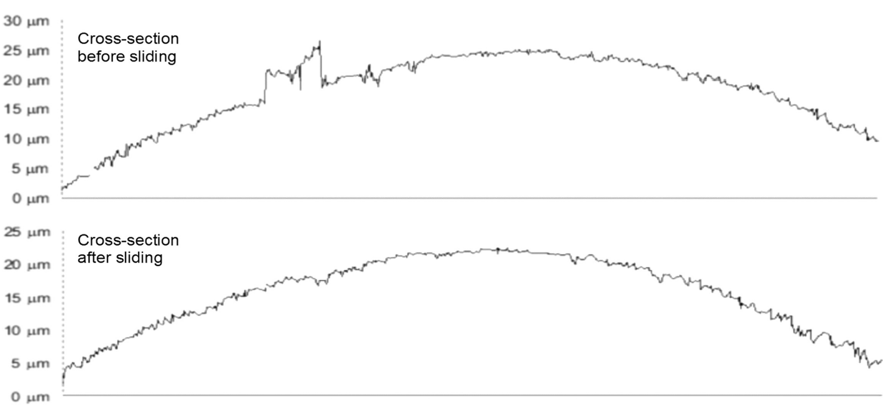

Fig. 1. Quantification of surface roughness damage due to shearing between two quartz particles: interferometer section before and after shearing (Senetakis et al., 2013c) – Horizontal size is 141.5 µm.

(vertical axis) with the removal of asperities due to shearing. This experimental observation may be one of the keys to the connection between the particle-contact response and the constant-state macro-scale properties of soils.

The higher magnitude of stiffness for soils of stronger-harder particles in comparison to weaker-crushable particles, found by Senetakis et al. (2012, 2013a) in their resonant column tests, along with the probable different energy dissipation mechanisms from small to medium strains, may be explained by the significant differences observed in the micromechanical tests by Senetakis et al. (2013c) at the contacts of strong and weak particles with respect to friction and stiffness on the micro-scale level. Previous research works, for example, Sadd et al. (1993, 2000), Sazzad and Suzuki (2011), Barreto and O' Sullivan (2012) or Huang et al. (2014), have highlighted through numerical studies the partially important effect of the particle contact characteristics (e.g., coefficient of friction at particle contacts, stiffness or particle-contact response model) in the overall macro-scale behavior of soils.

In this study a synthesis of torsional resonant column tests is presented on a potential fill–backfill material of hard grains with particle size from coarse sand to fine gravel and a variety of coefficients of uniformity. Particular focus is given to the constant-state properties of the samples in terms of the G_0–p' and D_{s0}–p' relationships in the range of relatively low confining stresses which represent typical low working loads for geotechnical engineering design. For this range of relatively low stresses, no measurable damage to particles was observed, at least visually. For further interpretations and a link between the macro-scale observed behavior of the samples and the probable effect of the particle contact response, additional dynamic test results that have been published by the authors were included and re-analyzed by means of investigating the G_0–p' relationship adopting formulae from the theory of elasticity.

2. Materials, sample preparation and testing program

2.1 Primary dynamic testing program: materials and experimental techniques

Fifteen samples, denoted as "SAMPLE01" to "SAMPLE15", were created in the laboratory from the same parent soil of hard, angular particles of low sphericity. The laboratory-created samples had a mean grain size, d_{50}, a coefficient of uniformity, C_u, and a maximum grain size, d_{max}, in the ranges of 1.33–10.1 mm, 1.03–12.5 and 2.00–12.7 mm, respectively. The specific gravity of solids was determined by adopting the water pycnometer method (ASTM, 2002, D854-02) with a value equal to 2.67, which was found independent of the particle size. Adopting the unified classification system USCS (ASTM, 2000a, D2487-00), the soils were classified as SP, SP-SW, GP and GW with varying percentages of sand and gravel portions. It is noted that by employing the ASTM specifications, the gravel-size grains were defined as the fraction retained on sieve No. 4 (size equal to 4.75 mm) and the "gravelly" samples for soils that had a gravel content of more than 50% of dry mass. These samples, presented in Fig. 2 and Table 1, comprised the materials of the primary dynamic testing program of the study and they were subjected to isotropic torsional resonant column (RC) testing in a dry state. The maximum void ratio (e_{max}) of the samples was determined following the ASTM (2000b) D4254-00 specification, whilst the vibratory table method (ASTM, 2000c, D4253-00) was used to determine the minimum void ratio (e_{min}). An optical microscope image of the fine-sand fraction of the parent soil is given in Fig. 3 (fraction 0.075–0.180 mm). Adopting the empirical chart for the quantification of the particle shape descriptors by Krumbein and Sloss (1963), it was revealed that the particles had very low roundness with R values between 0.1 and 0.3 and very low sphericity with S values between 0.3 and 0.5 for the majority of the particles. It is noted that R and S denote the mean roundness and the sphericity of the grains, respectively (Krumbein and Sloss, 1963; Santamarina et al., 2001; Cho et al., 2006).

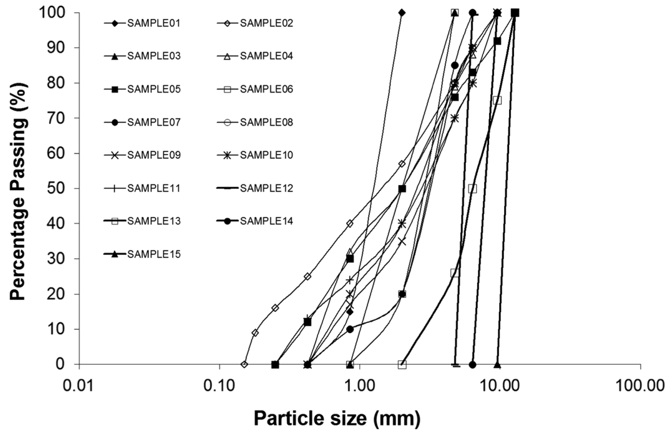

Fig. 2. Grain size distribution curves of materials tested in a Drnevich-type resonant column apparatus (primary dynamic testing program).

For each sample of the primary dynamic testing program, two specimens were constructed in a standard split mold, approximately 71 mm in internal diameter and 142 mm in height, one loose to very loose specimen and one dense to very dense specimen. To prepare the loose samples, the hand spooning method was used and the soil was prepared keeping a very small height of fall between the spoon and the free surface of the sample. For dense samples, the material was prepared in fourteen layers of, approximately, 10 mm in thickness. Compaction was applied for each layer using a stainless steel tamper with diameter about 0.6 times the diameter of the sample and a weight of about 9 kN. The height of drop of the tamper was approximately equal to 40 mm and the total number of tips for the fourteen layers was equal to approximately 1050 (i.e., on average 75 tips per layer). Assuming a diameter of the sample of 70 mm and a length of 140 mm, the applied compaction energy was about 700 kN m/m^3. This compaction energy is slightly greater than the energy provided in the specifications of ASTM for standard compaction (600 kN m/m^3) which resulted in high density

Table 1
Laboratory-created samples of primary dynamic testing program.

Laboratory material	d_{50} (mm)	C_u	C_c	d_{max} (mm)	e_{min}	e_{max}	Gravel content (%)	USCS	Method
(1)	(2)	(3)	(4)	(5)	(6)	(7)	(8)	(9)	(10)
SAMPLE01	1.33	2.13	1.01	2.00	0.502	0.876	0	SP	RC-T
SAMPLE02	1.33	11.8	0.68	9.53	0.271	0.511	20	SP-SW	RC-T
SAMPLE03	2.00	2.50	1.07	4.75	0.467	0.810	0	SP	RC-T
SAMPLE04	2.00	5.40	0.50	9.53	0.370	0.651	21	SP	RC-T
SAMPLE05	2.00	7.30	0.65	12.7	0.302	0.633	25	SP-SW	RC-T
SAMPLE06	3.07	1.53	0.90	4.75	0.572	0.950	0	SP	RC-T
SAMPLE07	3.00	2.45	1.10	6.35	0.465	0.818	15	SP	RC-T
SAMPLE08	3.07	4.24	1.77	9.53	0.362	0.654	20	SP	RC-T
SAMPLE09	2.90	5.95	1.19	9.53	0.450	0.880	30	SP-SW	RC-T
SAMPLE10	3.00	7.85	0.68	9.53	0.424	0.849	40	SP-SW	RC-T
SAMPLE11	3.00	12.5	0.94	9.53	0.330	0.590	40	SP-SW	RC-T
SAMPLE12	5.50	1.17	0.96	6.35	0.688	0.985	100	GP	RC-T
SAMPLE13	6.40	2.70	1.19	12.7	0.453	0.820	75	GW	RC-T
SAMPLE14	7.80	1.22	0.94	9.53	0.593	0.870	100	GP	RC-T
SAMPLE15	10.1	1.03	1.00	12.7	0.590	0.902	100	GP	RC-T

(2) Mean grain-size; (3) coefficient of uniformity;(4) coefficient of curvature; (5) maximum grain size
(6) minimum void ratio; (7) maximum void ratio;
(8) percentage of coarse soil retained on No. 4 (4.75 mm) sieve; (9) ASTM D2487-00;
(10) RC-T = resonant column torsional mode
Low-amplitude RC tests were performed at increasing steps of p' equal to 25, 50, 100 and 200 kPa.

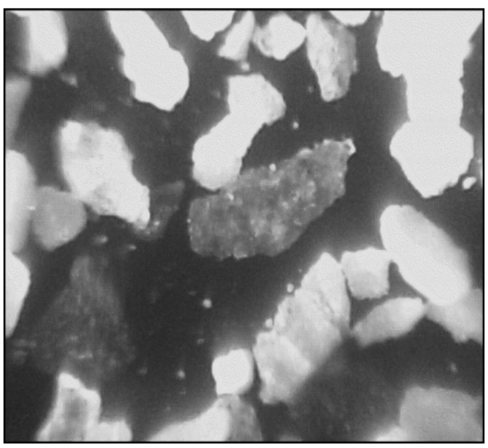

Fig. 3. Optical microscope image of fine-sand portion of granular material of primary dynamic testing program (fraction 0.075–0.180 mm).

samples. It is noted that the fractions of the study were coarse-grained, and thus, the difference in e_{max} and e_{min} is expected to be narrow (Menq, 2003). This is opposite to the trend observed in clays, for which soils small changes in the overconsolidation ratio can produce significant changes in the void ratio. Therefore, small changes in the compaction energy in the study, and thus, small changes in the void ratio at which the samples were prepared could reflect significant changes in the initial relative density, as depicted in Table 2.

For each specimen, prior to the first isotropic consolidation stage in the resonant column at $p' = 25$ kPa, a vacuum of 5 kPa was applied during the setup of the drive mechanism and the surrounding electrical and mechanical parts of the resonant column. After the setup of the apparatus, each sample was subjected to resonant column testing in torsional mode of vibration at increasing steps of p' equal to 25, 50, 100 and 200 kPa. The aim of the primary dynamic testing program was to (a) measure elastic moduli G_0, and material damping D_{s0} of the potential fill and backfill materials in the range of very small strains; (b) study the effects of isotropic effective stress p', void ratio e and grain size characteristics on the dynamic constant-state properties of the samples; (c) develop empirical-type equations that can be used for modeling the elastic properties of granular soils, in particular, coarse-sands and gravels of very low sphericity and angular grains. A link between the soil properties at the grain scale and the overall macro-scale response of the samples, and comparisons between the results of this study and those of previously published data are also discussed. Details of the specimens of the primary dynamic testing program, including the initial void ratio, the dry unit weight and the relative density at which the specimens were prepared, as well as the range in shear strain amplitudes at which G_0 and D_{s0} were measured (denoted as γ_{LA}), are summarized in Table 2. It is noted that for the relatively low pressures adopted in the study, no significant damage to the grains or breakage of the asperities was observed, at least visually. As mentioned in the studies by Senetakis et al. (2013a, 2013b), for crushable (volcanic) sands and gravels, some damage to the particles was observed visually after the resonant column tests. This was not the case for the hard particles included in the primary dynamic testing program of the present study.

The samples were vibrated in torsional mode using a fixed-free resonant column apparatus of the Drnevich type (Drnevich, 1967). This system utilizes four coils which surround the drive mechanism embedded with two magnets and an accelerometer to record the sample response on its top.

Table 2
Primary dynamic testing program.

Code name of specimen	e_o	γ_{do} (kN/m^3)	RD (%)	γ_{LA} ($\times 10^{-4}$%)	A^*_G (MPa)	n_G	A^*_D (%)	n_D
(1)	(2)	(3)	(4)	(5)	(6)	(7)	(8)	(9)
SAMPLE01-1[a]	0.594	16.43	75	4.4–4.6	71.7	0.63	0.78	−0.03
SAMPLE01-2[a]	0.820	14.39	15	6.2–9.6	64.7	0.65	0.61	−0.30
SAMPLE02-1	0.354	19.34	65	3.3–4.0	36.0	0.71	0.79	−0.21
SAMPLE02-2	0.498	17.49	5	3.4–6.8	41.6	0.72	0.65	−0.05
SAMPLE03-1[a]	0.553	16.87	75	2.0–3.7	63.5	0.57	0.53	−0.08
SAMPLE03-2[a]	0.770	14.80	12	6.3–7.0	65.4	0.67	0.62	−0.24
SAMPLE04-1	0.440	18.19	75	1.3–5.0	48.8	0.64	0.70	−0.05
SAMPLE04-2	0.605	16.32	16	4.4–7.5	56.5	0.68	0.69	−0.36
SAMPLE05-1	0.396	18.76	72	1.0–5.0	44.1	0.61	0.77	−0.09
SAMPLE05-2	0.558	16.81	23	4.5–7.9	50.7	0.67	0.71	−0.27
SAMPLE06-1	0.579	16.59	98	4.1–4.7	77.1	0.45	0.83	−0.02
SAMPLE06-2	0.835	14.27	30	5.2–7.5	73.5	0.55	0.61	−0.27
SAMPLE07-1	0.611	16.26	59	2.1–2.5	75.1	0.50	0.61	−0.12
SAMPLE07-2	0.718	15.25	28	2.3–5.2	77.7	0.47	0.96	−0.12
SAMPLE08-1	0.483	17.66	58	3.8–7.3	57.4	0.43	0.79	−0.12
SAMPLE09-1	0.479	17.71	93	2.8–4.2	66.0	0.65	0.57	−0.26
SAMPLE10-1	0.592	16.45	60	4.2–7.8	51.1	0.63	0.95	−0.16
SAMPLE11-1	0.448	18.09	55	1.4–4.4	51.8	0.59	0.65	−0.25
SAMPLE11-2	0.570	16.68	8	4.1–8.4	57.4	0.60	0.91	−0.19
SAMPLE12-1[b]	0.700	15.41	96	1.9–4.1	90.9	0.46	0.59	−0.10
SAMPLE12-2[b]	0.878	13.95	36	2.1–4.1	83.2	0.50	0.58	−0.18
SAMPLE13-1	0.633	16.04	51	3.9–4.2	89.3	0.48	0.74	−0.05
SAMPLE13-2	0.732	15.12	24	3.7–6.2	71.3	0.54	0.66	−0.30
SAMPLE14-1[b]	0.624	16.13	89	3.0–4.1	92.3	0.46	0.76	−0.19
SAMPLE14-2[b]	0.846	14.19	9	4.5–5.2	78.8	0.53	0.72	−0.16
SAMPLE15-1[b]	0.618	16.19	91	2.1–2.6	79.3	0.48	0.52	−0.25
SAMPLE15-2[b]	0.867	14.03	11	4.2–6.8	85.3	0.48	0.76	−0.27

(2) Initial void ratio; (3) initial dry unit weight; (4) initial relative density; (5) shear stain at which low-amplitude RC measurements were conducted; (6), (7) shear modulus constants; (8), (9) material damping constants.
[(a)]Senetakis et al. (2012, 2013a).
[(b)]Senetakis et al. (2013b).

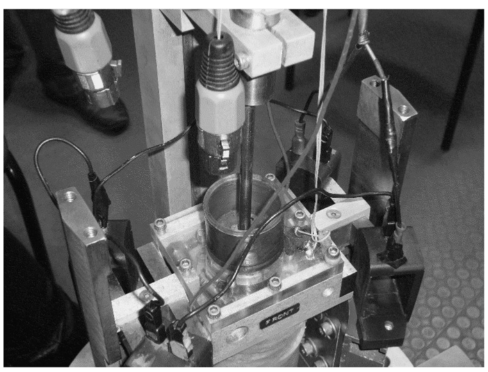

Fig. 4. Close-up view of top of sample, excitation mechanism and surrounding coils of the Drnevich-type resonant column used in the experiments of the primary dynamic testing program.

A close-up view of the top of the sample with the attached excitation mechanism and the surrounding coils is given in Fig. 4. The experiments were controlled and monitored manually through an electronic system of controllers, oscillator and amplifiers. Changes in sample height during the consolidation stage or during dynamic loading were monitored through a vertically positioned linearly variable differential transformer (LVDT) of repeatability equal to 0.01 mm. This means that the transducer could capture changes in the sample length not less than 0.01 mm. In those tests and for the case of dry specimens, the estimated changes in sample volume were implemented by the records of the vertically positioned LVDT assuming isotropic compression of the sample through Eq. (3), where ε_v and ε_a are the volumetric and axial strains, respectively.

$$\varepsilon_v = 3 \times \varepsilon_a \tag{3}$$

For the analysis of the resonant column tests, the ASTM specifications were adopted (ASTM, 1992), whilst for the material damping derivations, the steady-state vibration method was used (Senetakis et al., 2015).

2.2 Secondary dynamic testing program: analysis of literature test data

Apart from the samples of the primary dynamic testing program (Tables 1 and 2), additional granular soils, for which wave propagation velocities and moduli have been presented in previous published works by the authors, were included in the study. These soils are summarized in Table 3 and referred to as samples of the secondary dynamic testing program. Quartz sand SP-2 was studied by Madhusudhan (2011); this soil was subjected to torsional and flexural modes of vibration in a modified Stokoe-type resonant column apparatus (Cascante et al., 1998). Quartz sand SP-4 was studied by Kumar and Madhusudhan (2010); this soil was subjected to bender/extender element tests; and thus, shear and Young's moduli were measured for both SP-2 and SP-4. Details of the bender/extender element method and the adopted interpretations may be found elsewhere (e.g., Kumar and Madhusudhan, 2010, 2012). The soils with code names LWCID6 (pumice gravel) and V3 (rhyolitic crushed rock) in Table 3 were studied by Senetakis et al. (2012, 2013a, 2013b); these soils were subjected to a torsional mode of vibration under isotropic resonant column testing.

All the materials included in Table 3 were prepared at three to five initial void ratios; and thus, these samples were included in this study in order to (a) enrich the interpretations of this research work with respect to the effect of the preparation method and the initial fabric on the elastic modulus parameters, (b) highlight the importance of the particle contact response in the constant-state behavior of particulate media by comparing the effect of p' in the changes in void ratio in samples of variable types (i.e., hard or weak-crushable grains) and (c) provide, based on the experiments, useful equations that can be utilized in numerical simulations of particulate media (i.e., discrete element simulations) associated with changes in the void ratio of isotropically consolidated samples of variable types for a given change in p'. It is noted that sands SP-2 and SP-4 are quartz of strong-massive particles, whereas materials LWCID6 and V3 are volcanic soils of weaker particles of intra-particle voids. Therefore, the interpretations for those soils comprise the key for a link between properties at the grain scale and macro-scale observed responses associated with constant-state properties.

3. Experimental results and discussion

3.1 Small-strain shear modulus: formulation of empirical-type equation, typical results and comparisons with literature models

Typical plots of small-strain shear modulus G_0 against p' are given in Fig. 5(a) and (b) for uniform and well-graded samples, respectively. Fitting curves of the general formula of Eq. (1) are also depicted in these figures along with the computed values for the power n_G.

For the uniform soil (SAMPLE06), this power corresponded to values in a range of $n_G = 0.45–0.55$, which are typical values for reconstituted uniform granular soils reported in the literature (e.g., Hardin and Richart, 1963; Hardin, 1978; Kokusho, 1980; Santamarina et al., 2001). For the well-graded soil (SAMPLE04), n_G had higher values, which was the general trend for the well-graded soils of the study in comparison to uniform samples.

In Fig. 6, the measured G_0 values of the study were compared with empirical-type models proposed in the literature. In particular, the formulae proposed by Hardin and Richart (1963) in Fig. 6(a), Menq (2003) in Fig. 6(b) and Wichtmann and Triantafyllidis (2009) were used for this purpose. It was noticed that these formulae underestimated the measured shear moduli and this may be attributed in part to differences in the particle shape descriptors between the soils of the present study and the soils used for the development of the empirical-type models in previous studies. More pronounced scatter was noticed at higher levels of p' which mirrors the possible scatter of the n_G values. On the other hand, the underestimation of the shear moduli mirrors the differences in A_G values between the empirical models and the data of the study. In previous works, for example, by Menq (2003) or Wichtmann and Triantafyllidis (2009), the grading characteristics were incorporated into the development of the G_0 formulae, but it is possible that these formulae may more efficiently cover soils of sub-angular to rounded particles,

Table 3
Samples of secondary dynamic testing program.

Laboratory material	d_{50} (mm)	C_u	C_c	d_{max} (mm)	Gravel content (%)	USCS	Type	Method
(1)	(2)	(3)	(4)	(5)	(6)	(7)	(8)	(9)
SP2[a]	0.31	2.00	1.08	0.42	0	SP	Quartz	RC-T/F
SP4[b]	2.50	1.32	0.88	4.75	0	SP	Quartz	BE/EE
V3[c]	0.55	4.18	0.75	4.75	0	SP	Rhyolite	RC-T
LWC1D6[d]	5.60	1.20	0.97	9.53	96	GP	Pumice	RC-T

(2) Mean grain-size; (3) coefficient of uniformity; (4) coefficient of curvature; (5) maximum grain size;
(6) percentage of coarse soil retained on No.4 (4.75 mm) sieve; (7) ASTM D2487-00
(8) Type of soil;
(9) RC-T/F = resonant column torsional and flexural modes, RC-T = resonant column torsional mode BE/EE = bender and extender elements.
[(a)] Madhusudhan (2011).
[(b)] Kumar and Madhusudhan (2010).
[(c)] Senetakis et al. (2012, 2013a).
[(d)] Senetakis et al. (2013b).

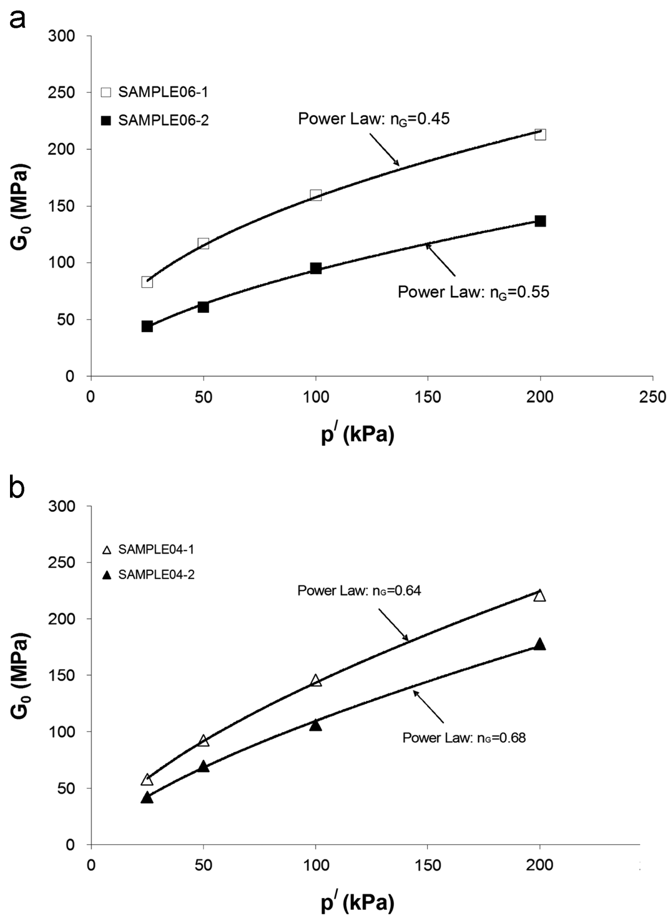

Fig. 5. Typical plots of shear moduli against isotropic effective stress for (a) uniform soil SAMPLE06 and (b) well-graded soil SAMPLE04.

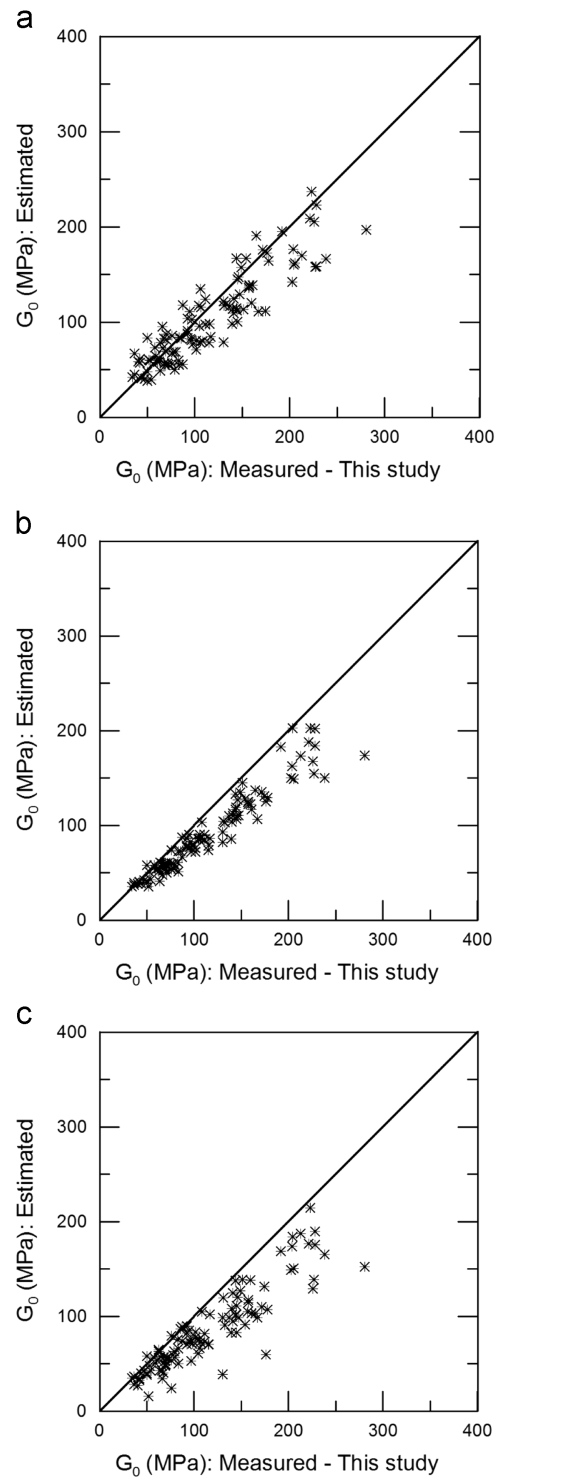

Fig. 6. Comparison between measured and estimated G_0 using formulae from the literature: (a) Hardin and Richart (1963), (b) Menq (2003) and (c) Wichtmann and Triantafyllidis (2009).

whilst in the present study, the grains were of high angularity. Cho et al. (2006) highlighted the importance of particle shape in both A_G and n_G parameters. Thus, a modification of the constants of those empirical formulae is necessary for a better fit to granular soils of high angularity.

3.2 Effect of isotropic pressure on changes in void ratio

In addition to the effect of C_u on the small-strain shear modulus parameters, the RC test results in Fig. 5 and for a given sample, showed higher values for n_G for a looser specimen than a denser one, and this was a systematic trend observed in the study. In order to further examine the effect of the sample preparation method on n_G, the changes in void ratio de, of the samples, due to the change in p', were estimated by adopting the formulae from the theory of elasticity expressed through Eqs. (4) and (5) (Richart et al., 1970). These formulae may provide an alternative estimation of the changes in sample void ratio due to an increase in p'. Typically, changes in void ratio are implemented by assuming isotropic compression.

$$\mathrm{de} = \frac{p' \times (1 + e_o)}{K} \tag{4}$$

$$K = E_0 - \frac{4}{3}G_0 \tag{5}$$

In Eqs. (4) and (5), K is the bulk modulus, e_o is the void ratio at which the samples were prepared, G_0 is the measured small-strain shear modulus and E_0 is the small-strain Young's modulus. For the computation of E_0, Eq. (6) was used by assuming a value for Poisson's ratio, equal to 0.25, which might be representative for granular soils (Menq, 2003).

$$E_0 = 2 \times (\nu + 1) \times G_0 \tag{6}$$

The change in void ratio de, for a given increase in p' for SAMPLE04 and SAMPLE06, is given in Fig. 7. Through a regression analysis, the fitting curves of the general formula of Eq. (7) were also plotted in the figure. Parameter n_e in Eq. (7) expresses the slope of the de–p' relationship, whilst β is a constant, and thus, n_e mirrors the alteration in constant-state properties of granular soils for a given change in p'.

$$\mathrm{de} = n_e \times p' + \beta \tag{7}$$

From the results in Fig. 7 it was demonstrated that the exponent n_e decreased with a decrease in void ratio or, alternatively, with an increase in relative density. These observations demonstrated that the power n_G, and thus, the G_0–p' relationship, is possibly affected by the preparation method, and that the more pronounced increase in G_0 with an increase in p', for a looser sample, is attributed to the more pronounced changes in void ratio when the sample has a lower relative density. This observed trend might be explained by the fundamental behavior of soils reported by Jovicic and Coop

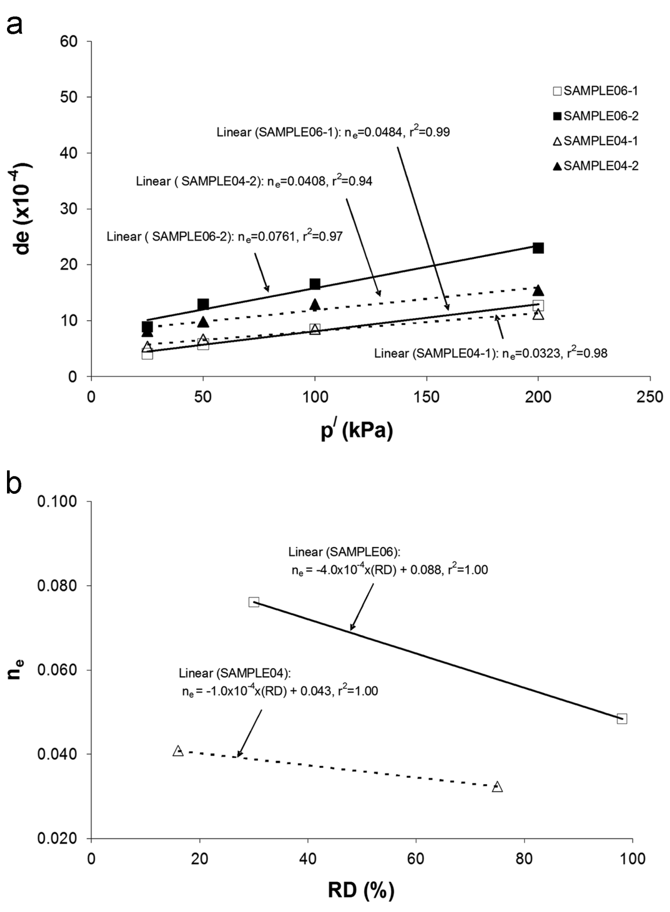

Fig. 7. Variation in (a) changes in void ratio de against p' and (b) exponent n_e against relative density RD for uniform SAMPLE06 and well-graded SAMPLE04.

(1997). In particular, Jovicic and Coop found that the samples they tested, prepared with different initial void ratios, tended to a unique line in the log G_0–log p' plot and this observed trend was more pronounced at relatively high isotropic pressures, in general beyond 1.0 MPa. In the present study and in most soil dynamics laboratory research works, the pressures under consideration are in the range of 0.05–0.5 MPa for most practical purposes. Therefore, the slight increase of n_G for a looser packing, may be related to the trend of the initial moduli at variable relative densities and for a given soil to converge at higher pressures to a unique line.

It is noted that, in this study, the investigation of the effect of the preparation method on the shear modulus parameters was limited because only two specimens were tested in the resonant column for each sample of the primary dynamic testing program, namely, a relatively dense to very dense sample prepared with compaction in layers and a loose to very loose sample prepared with the hand-spooning method. For the sake of completeness and in order to further study the aforementioned interpretations, the authors present herein corresponding results by Madhusudhan (2011) and Kumar and Madhusudhan (2010) who thoroughly investigated the effect of the sample preparation method on the shear modulus parameters of a fine-grained uniform quartz sand denoted as SP2 and a coarse-grained uniform sand denoted as SP4 (Table 3). The de–p' relationships from those two studies are presented in Figs. 8 (a) and 9(a) along with estimated fitting curves using Eq. (7). The n_e–RD relationships are plotted in Figs. 8(b) and 9(b). These results, in agreement with the findings of the primary dynamic testing program, demonstrated the importance of the sample preparation method in the G_0–p' relationship with a decrease of the power n_e for denser samples.

3.3 Effect of particle type and particle contact response on de–p' relationship

The importance of soil type and the nature of the particle contact response on the de–p' relationship was examined by a comparison between the results of Figs. 7–9 with the results shown in Fig. 10. In the latter figure, the corresponding de–p' and n_e–RD relationships for sands and gravels of volcanic origin with intra-particle voids are presented. The pumice soil, tested by Senetakis et al. (2013b), named LWC1D6 in that study, and the crushed rhyolithic rock, tested by Senetakis et al. (2012, 2013a), named V3 in their work, were subjected to torsional mode of vibration; and thus, only the G_0–p' relationships were available in ~~that study~~. The authors back-calculated Young’s modulus from Eq. (6) assuming a Poisson’s ratio of 0.25 for the volcanic soils. Using Eqs. (4)–(7) and through a regression analysis, the de–p' and n_e–RD relationships were thereafter determined. It was revealed that the values for n_e of the volcanic soils were much higher than the n_e values of the soils of this study (Fig. 7) and the studies by Madhusudhan (2011) (Fig. 8) and Kumar and Madhusudhan (2010) (Fig. 9) with additional substantially higher (de) values for the volcanic soils, in particular for the pumice gravel. For example, for the pumice gravel in Fig. 10, the n_e values ranged between 0.13

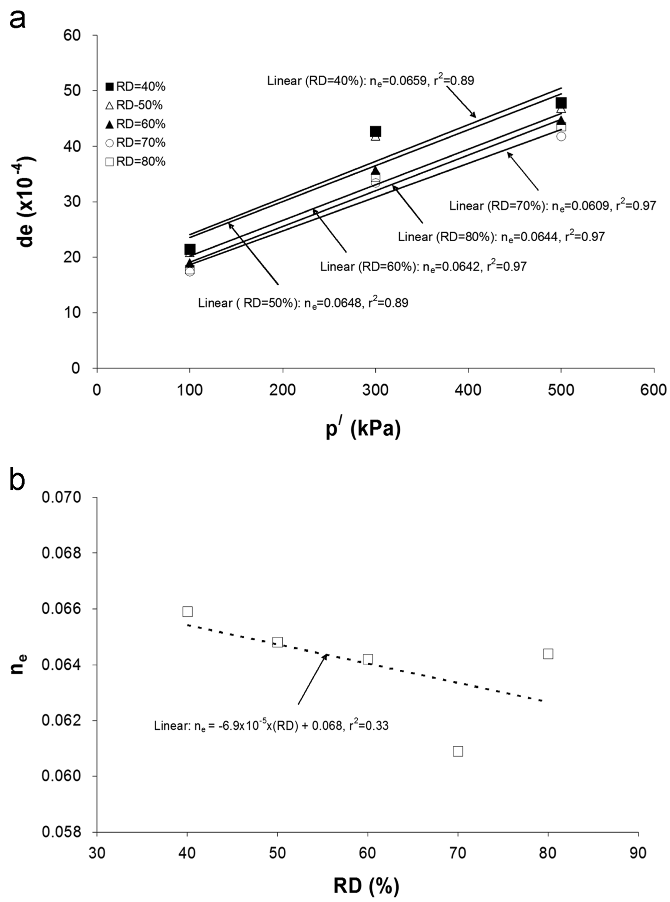

Fig. 8. Variation in (a) changes in void ratio de against p' and (b) exponent n_e against relative density RD for fine-grained uniform sand SP2 tested by Madhusudhan (2011) using torsional/flexural modes of vibration in a resonant column.

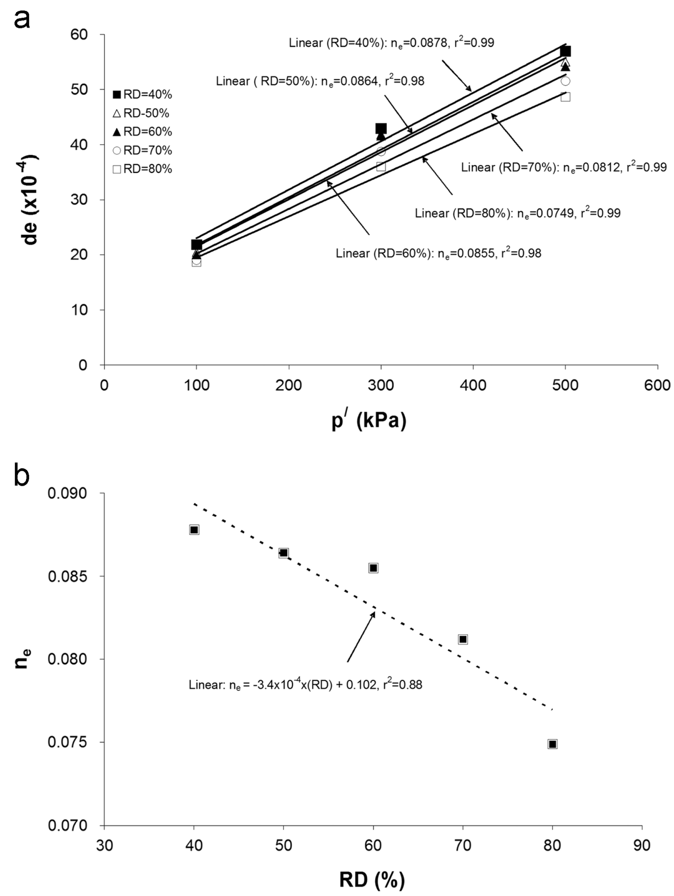

Fig. 9. Variation in (a) changes in void ratio de against p' and (b) exponent n_e against relative density RD for coarse-grained uniform sand SP4 tested by Kumar and Madhusudhan (2010) using bender/extender elements.

and 0.25, whereas for the soils of stronger particles tested by Madhusudhan (2011), Kumar and Madhusudhan (2010) or the samples of this study, the n_e values ranged between 0.04 and 0.09.

Consequently, along with the effect of the sample preparation method on the G_0–p' relationship, these interpretations highlighted the importance of soil type and particle contact response in the overall behavior of particulate media derived from dynamic element tests. These observations may be attributed, in part, to the plastic nature of the particle contact response in both the normal and tangential directions at the particle contacts. It is assumed, considering the recently acquired micromechanical test data by Cole et al. (2010) and Senetakis et al. (2013c, 2013d), that the response at the contacts of volcanic particles is more brittle with more pronounced damage to the grain surface which, in turn, mirrors the more pronounced fabric changes due to a change in p' in comparison to the assemblies of stronger particles. These observations may need to be considered when modeling the behavior of soils, for example, isotropically consolidated samples in discrete element analyses. Thus, the de–p' relationships in Figs. 7–10 may provide a link in this direction. It is noted that the more pronounced crushing for the volcanic grains is attributed primarily to the effect of the increase in isotropic pressure and not to the damage due to the sample preparation, which was verified by trial tests conducted when preparing the dense samples and by visually examining the possible damage to the grains due to compaction.

3.4 Development of empirical-type equations based on the primary RC testing program

In Fig. 11, the small-strain shear moduli are presented in log plots against p' for all samples of the primary dynamic testing program. For further analysis and interpretations for G_0, Eq. (8) was used, in which $F(e)$ is a void ratio function and p' is normalized with respect to the atmospheric pressure p_a. It is noted that parameter A_G^* in Eq. (8) is different in magnitude than parameter A_G in Eq. (1) because the effect of the void ratio is considered in the $F(e)$ function herein and p' is expressed by means of the normalized value p'/p_a. In Fig. 11, the samples have been separated into four groups; Fig. 11(a) refers to sands of $D_{50} \approx 1$ mm (Group A), Fig. 11(b) refers to sands of $D_{50} \approx 2$ mm (Group B), Fig. 11(c) refers to sands of $D_{50} \approx 3$ mm (Group C) and Fig. 11(d) refers to uniform, well-graded gravels (Group D).

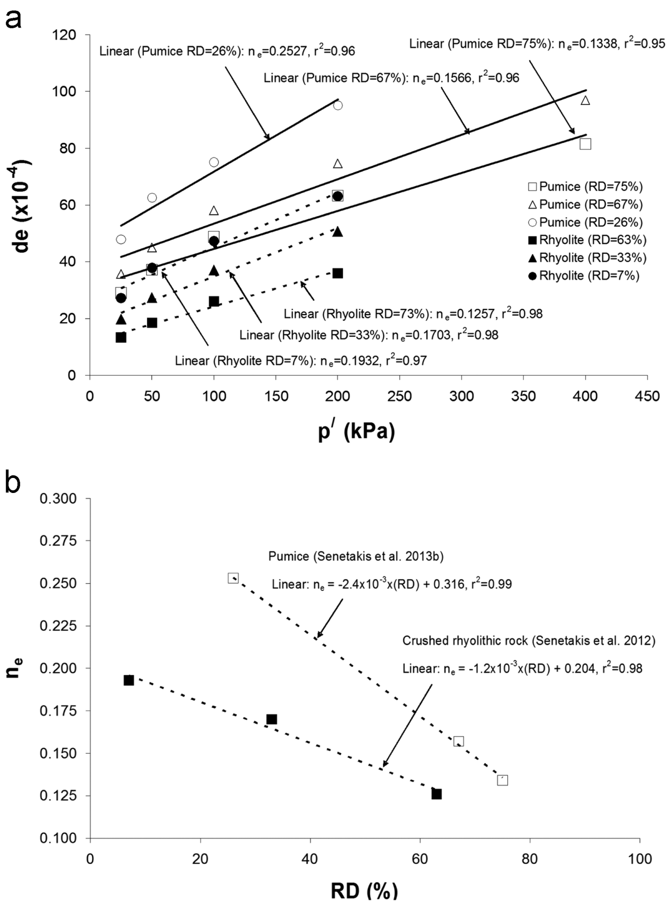

Fig. 10. Variation in (a) changes in void ratio de against p' and (b) exponent n_e against relative density RD for volcanic soils tested by Senetakis et al. (2012, 2013b) using torsional mode of vibration in a resonant column.

$$G_0 = A_G^* \times F(e) \times \left(\frac{p'}{p_a}\right)^{n_G} \tag{8}$$

$$F(e) = \frac{1}{e^{x_e}} \tag{9}$$

For $F(e)$, the general formula presented in Eq. (9) was used in which a value for the power x_e equal to 1.3 (after Jamiolkowski et al., 1991) was adopted. Therefore, Eq. (1) is rewritten as follows:

$$G_0 = A_G^* \times \frac{1}{e^{1.3}} \times \left(\frac{p'}{p_a}\right)^{n_G} \tag{10}$$

Using the experimentally derived G_0 values, the constants A_G^* and n_G were computed by fitting the G_0–p' relationship with the power-law type function. These values are summarized in Table 2. By plotting A_G^* and n_G against C_u, as shown in Fig. 12, fitting curves were estimated that correlated the small-strain shear modulus constants with the coefficient of uniformity. The proposed formulae are given in Eqs. (11) and (12).

$$A_G^* = -3.36 \times C_u + 81.8 \tag{11}$$

$$n_G = 0.485 \times C_u^{0.13} \tag{12}$$

For the shear moduli, the measured values are plotted against the predicted values in Fig. 13 using Eqs. (11) and (12). The scatter between the measured and the estimated values varied for most samples within a range of $\pm 20\%$ which is satisfactory for practical purposes. These formulae may be more applicable for coarse-grained materials of very low sphericity and high angularity grains as well as for the normalization of G/G_0 against shear strain curves, for example, by means of a hyperbolic type of model (Menq, 2003, Senetakis et al., 2013a, 2013b), since G_0 defines the plateau of the normalized curves. The scatter shown in Fig. 13 is significantly reduced in comparison to the results in Fig. 6, which is related, in part, to the variability in particle shape descriptors used in different research works to develop empirical-type models.

It is noted that, in Eq. (12), the relative densities of the samples were not incorporated into the n_G power due to the limited number of specimens prepared from each sample; and thus, the equation is applicable for relatively low engineering working loads. It is also noted that Eq. (12) would predict a value for n_G equal to approximately 0.49, for $C_u = 1$, which is very close to the typical value of 0.50 reported in the literature for the contact response of real-soil particles which, in nature, is visco-plastic to brittle. On the other hand, for $C_u = 5$, Eq. (12) would predict a value for n_G equal to 0.60. Similarly, previous research works have indicated an increase in n_G with an increase in C_u. In different studies, however, the different formulae and magnitudes of n_G mirror, in part, the differences in particle shape and overall morphology (for example, the research works by Menq, 2003, Wichtmann and Triantafyllidis, 2009, and the results of the present study). In particular, the empirical-type equations proposed by Menq (2003) and Wichtmann and Triantafyllidis (2009) for the n_G prediction as a function of C_u are plotted for comparison in Fig. 12(b).

On the other hand, Eq. (11) would predict a decrease in A_G^* with increasing C_u, which implies that for a given void ratio and p', the constant-state stiffness decreases in magnitude for well-graded soils. This observation may be analytically explained through Eq. (13), in which, f_n is the average contact force for an isotropic particulate medium of spherical particles of a given size, e is the void ratio, C_n is the average coordination number within the granular assembly, p is the isotropic pressure and r is the radium of the particles in contact (Rothenburg and Bathurst, 1989, after Cascante and Santamarina, 1996). This formula provides an indication and a strong link to the findings of this work on that, for a given e and pressure, the normal contact force, as an average value within a granular material, decreases with an increase in the coordination number and the latter is a function of the coefficient of uniformity.

$$f_n = \frac{4 \times \pi \times (1+e) \times r^2 \times p}{C_n} \tag{13}$$

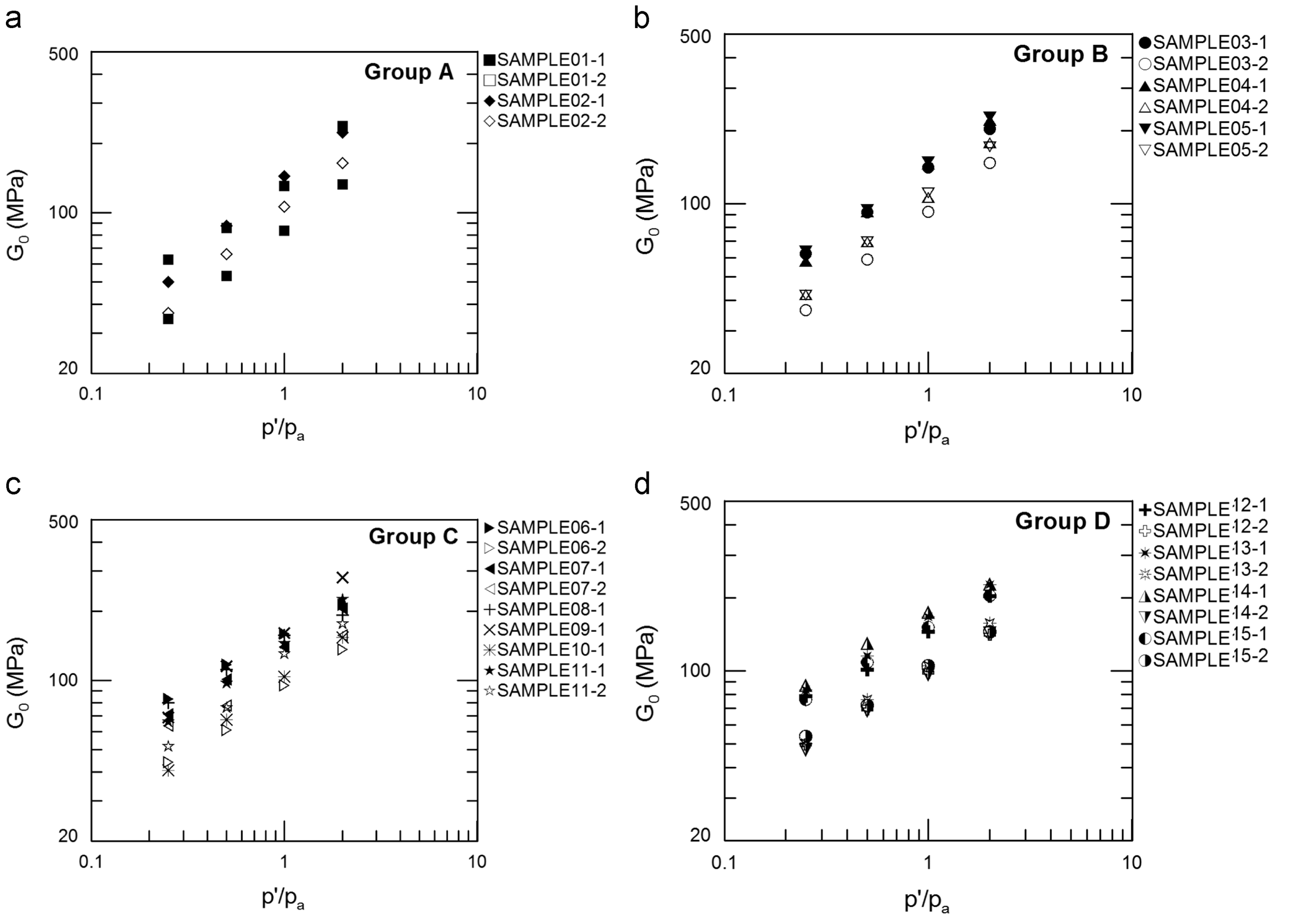

Fig. 11. Small-strain shear modulus against confining pressure normalized with respect to the atmospheric pressure of all specimens: (a) sands with $D_{50} \approx 1$ mm, (b) sands with $D_{50} \approx 2$ mm, (c) sands with $D_{50} \approx 3$ mm and (d) uniform and well-graded gravels.

3.5 Small-strain material damping: formulation and development of empirical equation

The measured small-strain material damping values of all samples of the primary dynamic testing program are plotted in Fig. 14 against the normalized pressure in log plots. A slight decrease in D_{s0} with an increase in pressure, which is consistent with previous research works (e.g., Cascante and Santamarina, 1996; Menq, 2003; Senetakis et al., 2012), was observed. For $p'=25$ kPa, material damping ranged between 0.80% and 1.10% for most samples, whilst for $p'=200$ kPa, D_{s0} ranged between 0.45% and 0.75% in the majority of the experiments. No clear trend was observed for the effect of the initial void ratio on D_{s0}; for example, for SAMPLE07 or SAMPLE15, D_{s0} values decreased for the denser specimens in comparison to the looser samples, but the opposite trend was observed for SAMPLE06 or SAMPLE14. It is noted that, in the study, the changes in sample volume, and thus, in void ratio, were based on the assumption of isotropic compression. In a previous study by Senetakis (2011), saturated samples at variable initial densities were tested and accurate measurements of changes in sample volume were incorporated. Senetakis (2011) did not notice a systematic effect of the void ratio on small-strain damping, which is in agreement with a previous work on granular soils by Menq (2003).

In order to further analyze the data, the following general formula for material damping was adopted which is given as a function of the normalized pressure.

$$D_{s0} = A_D^* \times \left(\frac{p'}{p_a}\right)^{n_D} \tag{14}$$

In Eq. (14), A_D^* and n_D are material constants. For those constants, a similar procedure to the one followed for the determination of the shear modulus constants was adopted. For each sample, D_{s0} was plotted against p'/p_a and a power law equation was determined expressed through the constant A_D^* and the power n_D. The analyses for those constants are summarized in Table 2, while in Fig. 15, A_D^* and n_D are plotted against the coefficient of uniformity. No clear trend was observed for the effect of the initial void ratio or the grading characteristics of the samples on D_{s0}. The data indicated an average value and a standard deviation for A_D^* and n_D equal to $0.71 \pm 0.12\%$ and -0.17 ± 0.10, respectively. The material damping constants were more scattered than the corresponding stiffness constants; this observation may be

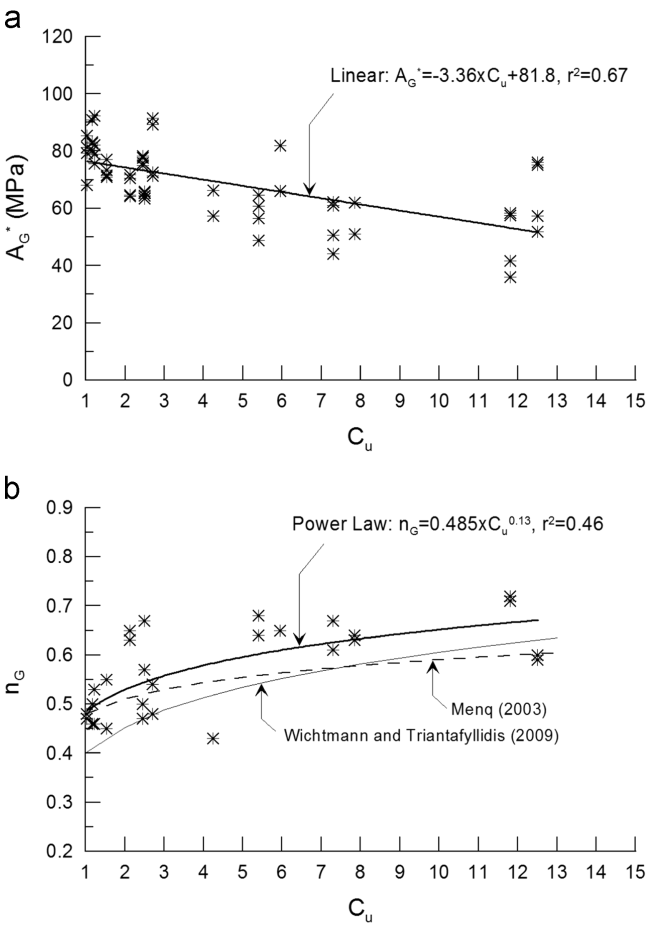

Fig. 12. Variation in shear modulus constants against coefficient of uniformity and comparisons with empirical-type models from the literature.

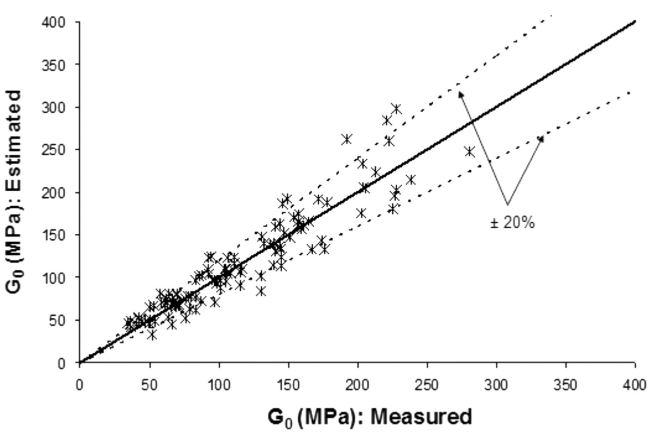

Fig. 13. Measured against estimated shear moduli.

attributed to the overall complex mechanisms of energy dissipation in particulate media at very small deformations. In their analyses, Senetakis et al. (2012), based on resonant column test data on fine to coarse grained sands of variable types including shape, mineralogy and morphology, similarly reported average values for the constant A_D^* between 0.62% and 0.52% for quartz and volcanic sands, respectively, whilst the n_G values were affected by particle shape. In Fig. 16, the measured against the estimated damping ratios using Eq. (14) are plotted. The use of Eq. (14) with $A_D^*=0.71\%$ and $n_D=-0.17$ did not show any systematic overestimation or underestimation of D_{s0} values over the measured damping ratios. For most data points, the scatter between the measured and estimated values varied within a range of $\pm 30\%$. This scatter is satisfactory considering the uncertainties in measuring material damping in the laboratory.

3.6 Practical implications of proposed formulae and future improvements

Computer codes for seismic response analysis studies use G_0 (or shear wave velocity V_s) and non-linear curves, i.e., modulus degradation and increase in damping against shear strain, as input. In addition, G_0 is important in the normalization of the G/G_0-strain curves which are very popular in engineering practice particularly when equivalent linear analysis codes are used for seismic response studies and in medium-strain geotechnical problems. G_0 is the "start point" of a normalized curve and it has been recognized for its importance in the prediction of deformations for both static and dynamic loading problems (e.g., Jovicic and Coop, 1997). Consequently, the importance of small-strain stiffness is associated not only with studies that include seismic loading, but also with conventional foundation engineering, tunneling design, infrastructures such as retaining walls and other facilities with fill–backfill material. Damping in the range of small-strains can also be very important in particular in small-strain problems which may be of interest in machine foundation vibration analyses and soil-structure-interaction analyses of dynamically loaded systems. Small-strain damping is also important for the geophysical characterization of sediments (Cascante et al., 1998). This means that the dynamic properties examined in the study are of immediate interest in engineering practice, including deformation prediction and dynamic problems, and the produced formulae of the paper can be used directly for predictions of ground deformation as well as for geophysical characterizations of sediments.

The aim of the study was to propose formulae for small-strain stiffness and damping prediction that are applicable to soils of similar characteristics in terms of particle size, distribution, specific gravity and most importantly particle shape descriptors, i.e., for soils of low sphericity and roundness. This type of soil, such as crushed rock, is very common in geotechnical projects.

It is noted that in the present study and, in particular, for stiffness derivations, a void ratio function proposed in the literature was incorporated, i.e., $F(e)=e^{-x}$ where the power x was equal to 1.3. In previous studies, for example by Menq (2003) or Senetakis et al. (2012), the experimental data were adjusted in order to compute a best-fit x power, but in the present work a constant value was adopted, without adjustment based on the specific experiments of the study. This may add some additional scatter to the predicted stiffness values. The decision for an appropriate void ratio function $F(e)$ to be used in the analysis affects the magnitude of the constant A_G, but it

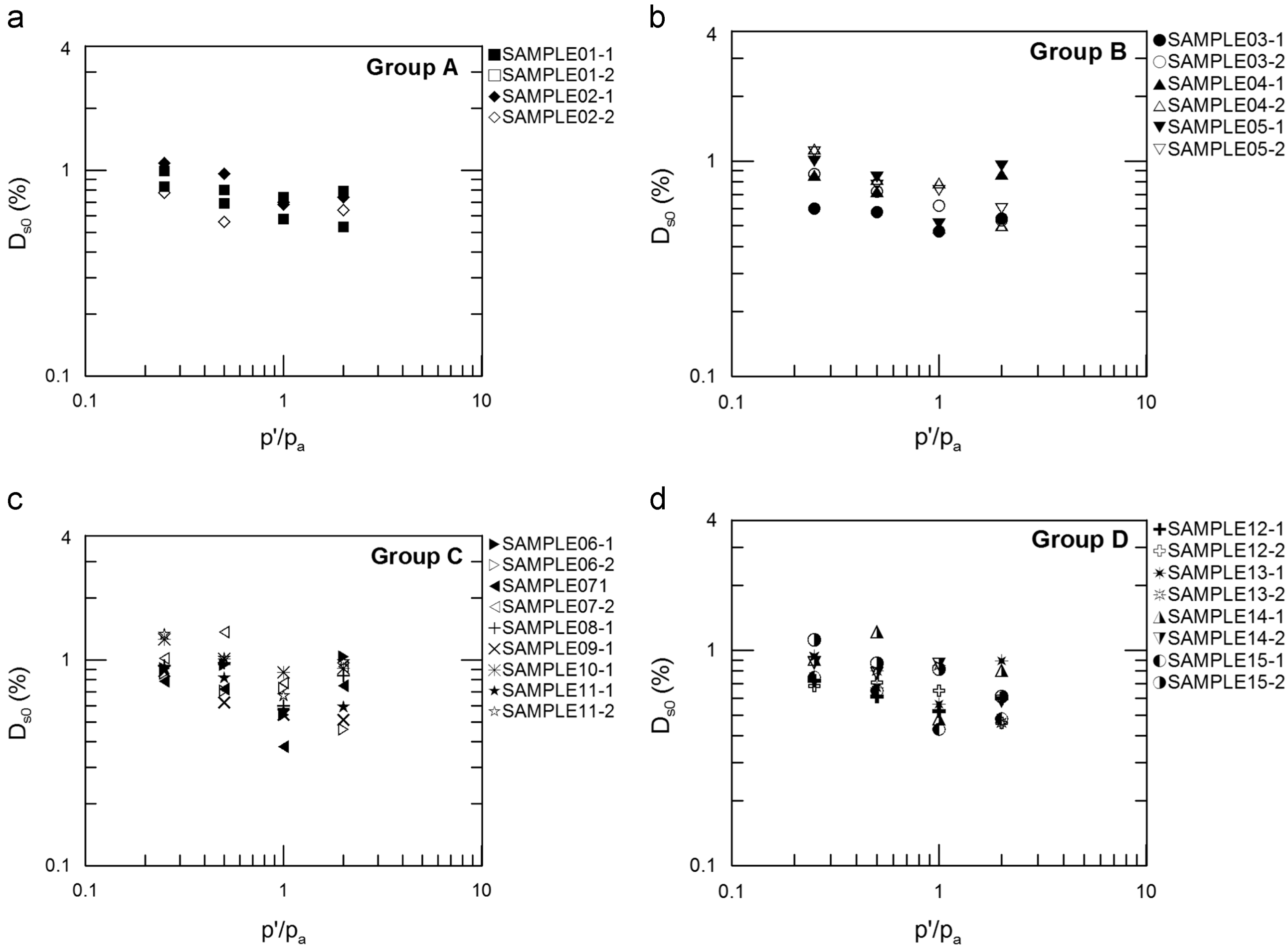

Fig. 14. Material damping values against confining pressure normalized with respect to atmospheric pressure of all specimens: (a) sands with $D_{50} \approx 1$ mm, (b) sands with $D_{50} \approx 2$ mm, (c) sands with $D_{50} \approx 3$ mm and (d) uniform and well-graded gravels.

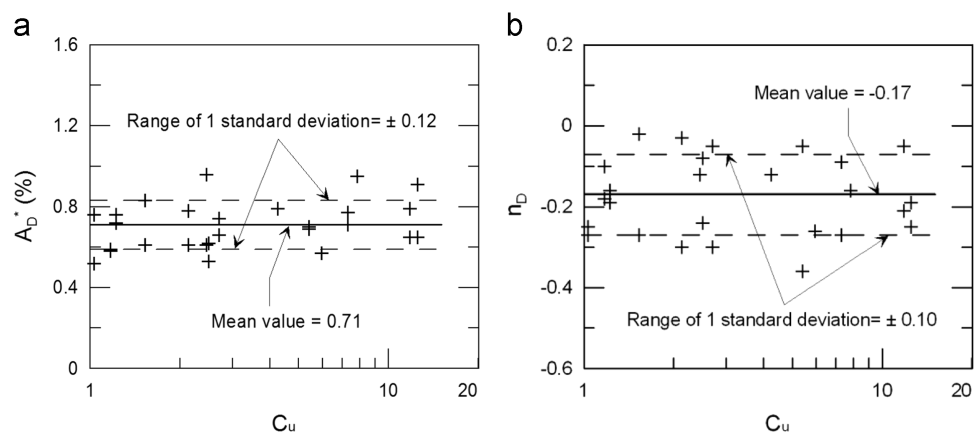

Fig. 15. Variation in material damping constants against coefficient of uniformity.

is expected not to have a qualitatively important effect on general trends, for example, the effect of C_u on the power n or the constant A_G, whilst the produced formulae demonstrated an improvement between the estimated and the measured values. It was out of the scope of this paper to investigate in further detail the uncertainties in estimating stiffness at small strains, which may include, for example, the effect of different void ratio functions to be used in the small-strain stiffness formula. The main contributions of this work were (1) to emphasize some differences with the literature data, for example, between different formulae for stiffness prediction; (2) to highlight the important effect of particle shape which significantly affects the differences in the proposed formulae in the literature; (3) to improve the general formula for G_0 prediction for the

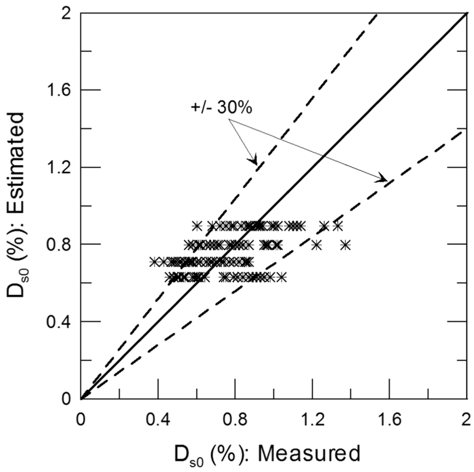

Fig. 16. Measured against estimated material damping.

particular type of soil which was mirrored through the improved comparison between the measured and the estimated values; and (4) to provide micro-mechanical interpretations and the effect of the particle contact response including soils of variable types.

4. Conclusions

The study presented a synthesis of torsional resonant column tests on a potential fill–backfill material with focus on elastic moduli G_0 and material damping D_{s0}. Additional previously published tests that adopted dynamic test methods were re-analyzed. The following main conclusions may be drawn:

1. The G_0–p' relationship followed a power law with observed effects of the preparation method and the coefficient of uniformity on the power n_G. These effects were attributed, in part, to the fundamental behavior of soils of convergent moduli with respect to the effect of the preparation method and to the effect of the coordination number on the magnitude and the distribution to the particle contact forces within a granular assembly, with respect to the coefficient of uniformity.

2. Using formulae from the theory of elasticity, along with previously published data from dynamic element tests, the importance of particle type and particle contact response was examined in terms of the changes in void ratio for a given change in p'. The more brittle in nature particle-contact response of weaker particles, such as volcanic soils, led to more pronounced changes in void ratio, and thus, changes in fabric with an increase in p', which in turn affected the G_0–p' relationship.

3. Material damping constants were more scattered and the effect of grading or the preparation method on D_{s0} was not clear. For the range of isotropic effective stresses in this study, small-strain material damping was generally found to be less than unity in magnitude, with a slight decrease with an increase in p'.

4. The developed equations of this research work may be directly used to model the behavior of potential fill–backfill materials which may find many applications in geotechnical engineering practice. These formulae may be more applicable to granular soils of very high angularity and very low sphericity. However, it is believed that further laboratory and theoretical research, by means of numerical simulations of granular assemblies, is necessary in order to examine some observed trends of this work. For example, the effect of the sample preparation method and its link to the magnitude and the distribution of particle contact forces, attenuation at the contacts of the soil particles and its link to the macro-scale observed material damping, or, the effects of particle shape and morphology in the energy dissipation mechanisms and stiffness of particulate media, need to be investigated.

Acknowledgments

The authors would like to thank the anonymous reviewers for their constructive comments and their detailed suggestions which helped us to improve the quality of the paper.

References

ASTM, 1992. Standard test methods for modulus and damping of soils by the resonant column method: D4015-92, Annual Book of ASTM Standards. ASTM International.

ASTM, 2000a. Standard practice for classification of soils for engineering purposes (Unified Soil Classification System): D2487-00, Annual Book of ASTM Standards. ASTM International.

ASTM, 2000b. Standard test methods for minimum index density and unit weight of soils and calculation of relative density: D4254-00, Annual Book of ASTM Standards. ASTM International.

ASTM, 2000c. Standard test methods for maximum index density and unit weight of soils using a vibratory table: D4253-00, Annual Book of ASTM Standards. ASTM International.

ASTM, 2002. Standard test methods for specific gravity of soil solids by water pycnometer: D854-02, Annual Book of ASTM Standards. ASTM International.

Barreto, D., O' Sullivan, C., 2012. The influence of inter-particle friction and the intermediate stress ratio on soil response under generalised stress conditions. Granul. Matter 14, 505–521.

Cascante, G., Santamarina, C., 1996. Interparticle contact behavior and wave propagation. J. Geotech. Geoenviron. Eng. 122, 831–839.

Cascante, G., Santamarina, C., Yassir, N., 1998. Flexural excitation in a standard torsional-resonant column. Can. Geotech. J. 35, 478–490.

Cavarretta, I., Coop, M.R., O' Sullivan, C., 2010. The influence of particle characteristics on the behavior of coarse grained soils. Geotechnique 60 (6), 413–423.

Cho, G.-C., Dodds, J., Santamarina, C., 2006. Particle shape on packing density, stiffness, and strength. J. Geotech. Geoenviron. Eng. 132, 591–602.

Chung, R., Yokel, F., Drnevich, V., 1984. Evaluation of dynamic properties of sands by resonant column testing. Geotech. Test. J. 7 (2), 60–69.

Cole, D.M., Peters, J.F., 2007. A physically based approach to granular media mechanics: grain-scale experiments, initial results and impications to numerical modeling. Granul. Matter 9, 309–321.

Cole, D.M., Peters, J.F., 2008. Grain-scale mechanics of geologic materials and lunar simulants under normal loading. Granul. Matter 10, 171–185.

Cole, D.M., Mathisen, L.U., Hopkinks, M.A., Knapp, B.R., 2010. Normal and sliding contact experiments on gneiss. Granul. Matter 12, 69–86.

Drnevich, V., 1967. Effects of Strain History on the Dynamic Properties of Sand (Ph.D. Dissertation). University of Michigan.

Goto, S., Syamoto, Y., Tamaoki, S., 1987. Dynamics properties of undisturbed gravel samples obtained by the in situ freezing method. In: Proceedingsof the 8th Asian Regional Conference on Soil Mechanics and Foundation Engineering. Kyoto.

Hardin, B.O., Richart, F.E., 1963. Elastic wave velocities in granular soils. J. Soil Mech. Found. Div. 89, 33–65.

Hardin, B., 1978. The nature of stress strain behaviour of soil. In: Proceedings of the Geotechnical Division Speciality Conference on Earthquake Engineering and Soil Dynamics. ASCE, Pasadena, CA, vol. 1, pp. 3–90.

Huang, X., Hanley, K.J., O'Sullivan, C., Kwok, C.Y., 2014. Exploring the influence of interparticle friction on critical state behaviour using DEM. Int. J. Numer. Anal. Methods Geomech. 38, 1276–1297.

Jamiolkowski, M., Leroueil, S., Lo Priesti, D., 1991. Design parameters from theory to practice. In: Proceedingsof the International Conference on Geotechnical Engineering for Coastal Development: Geo-Coast 1991. Coastal Development Institute of Technology, Yokohama, Japan, pp. 877–917.

Jovicic, V., Coop, M.R., 1997. Stiffness of coarse-grained soils at small strains. Geotechnique 47 (3), 545–561.

Kokusho, T., 1980. Cyclic triaxial test of dynamic soil properties for wide strain range. Soils Found. 20 (2), 45–60.

Krumbein, W., Sloss, L., 1963. Stratigraphy and Sedimentation. W.H. Freeman and Company, San Francisco.

Kumar, J., Madhusudhan, B.N., 2010. Effect of relative density and confining pressure on Poisson ratio from bender and extender elements. Geotechnique 60 (7), 630–634.

Kumar, J., Madhusudhan, B.N., 2012. Dynamic properties of sand from dry to fully saturated states. Geotechnique 62 (1), 45–55.

Madhusudhan, B.N., 2011. Dynamic Properties of Dry to Fully Saturated States Using Resonant Column and Bender Element Tests (Ph.D. Dissertation). Indian Institute of Science, Bangalore, India.

Menq, F.-Y., 2003. Dynamic Properties of Sandy and Gravelly Soils (Ph.D. Dissertation). University of Texas at Austin, Austin, TX, USA.

Menq, F.-Y., Stokoe, K., 2003. Linear dynamic properties of sandy and gravelly soils from large-scale resonant tests. In: Di Benedetto, H., Doanh, T., Geoffroy, H., Sauzeat, C. (Eds.), Deformation Characteristics of Geomaterials. Swets and Zeitlinger, Lisse, pp. 63–71.

Radjai, F., Wolf, D., Jean, M., Moreau, J.-J., 1998. Bimodal character of stress transmission in granular packing. Phys. Rev. Lett. 80 (1), 61–64.

Radjai, F., Wolf, D., 1998. Features of static pressure in dense granular media. Granul. Matter 1, 3–8.

Richart, F.E., Hall, J.R., Woods, R.D., 1970. Vibrations of Soils and Foundations. Prentice Hall, Englewood Cliffs, 414.

Rothenburg, L., Bathurst, R.J., 1989. Analytical study of induced anisotropy in idealized granular material. Geotechnique 39 (4), 601–614.

Sadd, M.H., Tai, Q.M., Shukla, A., 1993. Contact law effects on wave propagation in particulate materials using distinct element modeling. Int. J. Non-Linear Mech. 28 (2), 251–265.

Sadd, M.H., Adhikari, G., Cardoso, F., 2000. DEM simulation of wave propagation in granular materials. Powder Technol. 109, 222–233.

Santamarina, C., Cascante, G., 1996. Stress anisotropy and wave propagation: a micromechanical view. Can. Geotech. J. 33, 770–782.

Santamarina, C., Cascante, G., 1998. Effect of surface roughness on wave propagation parameters. Geotechnique 48 (1), 129–136.

Santamarina, C., Klein, K., Fam, M., 2001. Soils and Waves. John Wiley and Sons, New York.

Sazzad, Md.M., Suzuki, K., 2011. Effect of interparticle friction on the cyclic behavior of granular materials using 2D DEM. J. Geotech. Geoenviron. Eng. 137 (5), 545–549.

Senetakis, K., 2011. Dynamic Properties of Granular Soils and Mixtures of Typical Sands and Gravels with Recycled Synthetic Materials (Ph.D. dissertation). Department of Civil Engineering: Aristotle University of Thessaloniki, Greece (in Greek).

Senetakis, K., Anastasiadis, A., Pitilakis, K., 2012. The small-strain shear modulus and damping ratio of quartz and volcanic sands. Geotech. Test. J. 35 (6)http://dx.doi.org/10.1520/GTJ20120073.

Senetakis, K., Anastasiadis, A., Pitilakis, K., 2013a. Normalized shear modulus reduction and damping ratio curves of quartz sand and rhyolitic crushed rock. Soils Found. 53 (6), 879–893.

Senetakis, K., Anastasiadis, A., Pitilakis, K., Coop, M., 2013b. The dynamics of a pumice granular soil in dry state under isotropic resonant column testing. Soil Dyn. Earthq. Eng. 45, 70–79.

Senetakis, K., Coop, M., Todisco, M.C., 2013c. The tangential load-deflection behaviour at the contacts of soil particles. Geotechnique Lett. 3 (2), 59–66.

Senetakis, K., Coop, M., Todisco, M.C., 2013d. The inter-particle coefficient of friction at the contacts of Leighton Buzzard sand quartz minerals. Soils Found. 53 (5), 746–755.

Senetakis, K., Coop, M.R., 2014. The development of a new micro-mechanical inter-particle loading apparatus. Geotech. Test. J. 37 (6), 1028–1039.

Senetakis, K., Coop, M.R., 2015. Micro-mechanical experimental investigation of grain-to-grain sliding stiffness of quartz minerals. Exp. Mech. 55 (6), 1187–1190. http://dx.doi.org/10.1007/s11340-015-0006-4.

Senetakis, K., Anastasiadis, A., Pitilakis, K., 2015. A comparison of material damping measurements in resonant column using the steady-state and free-vibration decay methods. Soil Dyn. Earthq. Eng. 74, 10–13.

Tanaka, Y., Kudo, K., Yoshida, Y., Ikemi, M., 1987. A Study on the Mechanical Properties of Sandy Gravel-dynamic Properties of Reconstituted Sample (Report U87019). Central Research Institute of Electric Power Industry (in Japanese).

Wichtmann, T., Triantafyllidis, T., 2009. On the influence of the grain size distribution curve of quartz sand on the small strain shear modulus $G_{\max}$. J. Geotech. Geoenviron. Eng. 135 (10), 1404–1418.

Yoshimine, M., Ishihara, K., Vargas, W., 1998. Effects of principal stress direction and intermediate principal stress on undrained shear behavior of sand. Soils Found. 38 (3), 179–188.